Novelty Journals

ISSN 2394-7349

International Journal of Novel Research in Engineering and Science
Vol. 9, Issue 2, pp: (35-39), Month: September 2022 - February 2023, Available at: www.noveltyjournals.com

The Relative Sensitivity of Rotor Impedance Parameters to the Design Changes in Rotor Bar Geometry - A Torque Production perspective

Nelson Oyakhilomen Omogbai

Electrical Engineering Department, Nnamdi Azikiwe University, Awka, Anambra State, Nigeria.

DOI: https://doi.org/10.5281/zenodo.7612848

Published Date: 06-February-2023

Abstract: **This article delves into the geometry-impedance relation of the three-phase squirrel cage induction motor (SCIM), to study the levels of sensitivity of the impedance parameters to design modifications in the geometry of the rotor bar cross section. Studies have long clarified the facts about the strong influence that the geometry of the rotor bar transverse section has on the standstill and operating impedance values of the rotor circuit, and it is a well-known fact that the development of electromagnetic torque as well as the shape of the torque-speed characteristic of the SCIM are all to a large extent dependent on the rotor circuit impedance. During design and optimization routines, the design engineer usually leverages on the aforementioned facts to accomplish a successful torque optimization program. Barring the saturation of the leakage flux path during large slip motoring operation, the magnitude of the rotor leakage reactance is usually greater than that of the rotor resistance, but the result of this study shows that the relative sensitivity of this reactance to design changes in the geometry of the rotor bar cross section, appears inferior.**

Keywords: **Rotor bar, Rotor leakage reactance, Rotor resistance, Design, Torque, Sensitivity.**

I. INTRODUCTION

Torque production in the three phase squirrel cage induction motor (SCIM) involves the interaction of the air gap flux with the rotor MMF. To a first order of approximation, the air gap flux is a function of the applied voltage and, hence, does not vary widely over a change in mechanical load. The second quantity, namely the rotor MMF, varies with the rotor (and therefore usually stator) current and hence has a much more dominant role in torque production. The stator and rotor currents, are, in turn, primarily a function of the impedance of the machine. In particular, key performance characteristics such as starting torque, and inrush current depend critically upon the leakage inductances together with the resistances [1].

The speed-torque characteristic can be modified by changing the rotor slot shape. This changes the resistance and reactance as a function of rotor frequency. A rotor slot shape that is deep and narrow, sometimes called deep bar, allows considerable magnetic flux to cross the slot. At standstill, the rotor current is at stator line frequency. The flux linkages, due to this high frequency current, distort the current density in the rotor to the top of the rotor bar, increasing its effective resistance [2]. It was stressed in [3] that for single cage induction motors and with one conductor in the slot, the skin effects increase with the slot (conductor) height, for given slip frequency. The slot leakage flux distribution depends notably on slot geometry and less on teeth and back core saturation.

The authors in [4] made it clear that by using suitable shapes and arrangements for rotor bars, it is possible to design squirrel-cage rotors so that their effective resistance at start is several times their resistance at low slip. This results from the inductive effect of the slot-leakage flux on the current distribution in the rotor bars, a concept known as the skin effect. The greater

Novelty Journals

ISSN 2394-7349

International Journal of Novel Research in Engineering and Science
Vol. 9, Issue 2, pp: (35-39), Month: September 2022 - February 2023, Available at: www.noveltyjournals.com

the rotor resistance is, the greater the torque will be for a given locked rotor current. However, if the rotor bar resistance is doubled, the locked rotor torque will not be doubled since the rotor slot impedance, which is the sum of rotor slot resistance and reactance, will increase with rotor bar resistively, thereby decreasing locked rotor current and therefore torque. Also, the depth of penetration of the current in the rotor bar due to the skin effect increases with increasing resistance [5].

It was emphasized in [7] that under blocked rotor condition, deep bar effect occurs, the total machine impedance is dominated by reactances and there is a rise in blocked rotor current. The deep bar effect causes an increase in the ratio of ac to dc resistance of the bar and the effective bar depth in producing the slot leakage permeance is reduced. Also, under the blocked rotor condition, the cross slot mmf increases in the same proportion as the current, resulting in large increases in leakage flux which attains its maximum value near the top of the slot causing tooth tip saturation (uncommon in open slots). Slot width increases in the region where tooth tip saturation occurs while the overall slot permeance decreases as a result. This decreases the slot leakage flux and thus the leakage reactance of the stator or rotor. Slot leakage flux increases with tooth saturation and decreases with tangentially wide slots [8].

As the bar becomes longer, the amount of flux linking to the bar increases, which increase the rotor copper loss during operation. The operating efficiency becomes poor if the rotor bar becomes small, because a small rotor resistance reduces the output. Since the skin effect mainly affects the upper portion of the bar, the area of this portion is reduced to increase the resistance at starting and so that the rotor copper loss is not so large [6]. An induction motor designer is forced to compromise between the conflicting requirements of high starting torque and good efficiency. Also, the peak torque actually occurs at a slip at which the rotor inductive reactance is equal to the rotor resistance, so the motor designer can position the peak torque at any slip by varying the reactance to resistance ratio [9].

This study therefore aims to further arm the SCIM designer with the knowledge of the relative sensitivity of the rotor impedance parameters to the design modifications made to the cross section of the rotor bar, should any delicate torque refinement procedure (or other impedance dependent finetuning) become necessary during design/optimization.

II. EXPERIMENTAL SET UP

The study was conducted at a frequency of 50Hz and 400V L-L with two squirrel cage induction motors (SCIM) rated 100 HP (M1) and 75HP (M2) which were run in Matlab. Two machines being used here mainly for corroborative purposes. The rotor bar shapes and specifications of the machines are given in fig 1 and table 1 respectively. In [10, 11] it was established that one of the influential geometries of the rotor bar cross section that govern the level of the slot leakage reactance (X_2) is the angle of taper (T). The bar top width (W) was also seen to strongly influence the level of the rotor resistance (R_2). Therefore, in this study these geometries were varied in small incremental steps, and the corresponding effect on the impedance parameters was tracked, noted and analyzed.

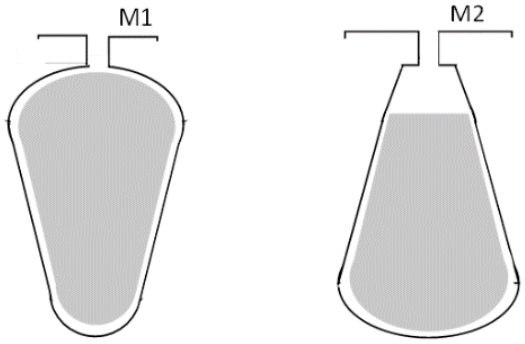

Fig 1: Rotor bar shapes.

TABLE I: Machine specifications

Paramaters	M1	M2
Number of poles (p)	8	6
Number of rotor slots (Sr)	55	55
Number of stator slots (Ss)	72	72
Full load efficiency (EffR) %	91.12268	91.01281
Full load current (I1R) Amps	137.6654	104.0402
Full load power factor (PFR)	0.858292	0.851315
Full load speed (nmR) rpm	738.5339	988.1062
Full load torque (TTdR) N.m	972.3505	545.2107
Starting Torque (Tst) N.m	1211.621	1033.852
Maximum Torque (Tmax) N.m	3368.963	2406.64
X1 (ohms)	0.119191	0.109422
X2pr (ohms)	0.132793	0.136917
Xm (ohms)	3.939174	4.741772
R1 (ohms)	0.035604	0.055372
R2pr (ohms)	0.042764	0.049827
Rc (ohms)	110.508	157.5086

Novelty Journals

ISSN 2394-7349

International Journal of Novel Research in Engineering and Science
Vol. 9, Issue 2, pp: (35-39), Month: September 2022 - February 2023, Available at: www.noveltyjournals.com

III. RESULTS AND DISCUSSION

Many publications abound of the influence of the rotor bar geometry on the rotor impedance as buttressed by more recent work in [10 & 11] as well as the SCIM design equations for deriving the equivalent circuit parameters outlined in [2 & 13]. As earlier alluded to in the introductory section, figs 2 and 3 echo the fact that the impedance parameters i.e., R_2 and X_2 are both critical to the determination of the SCIM starting performance, including the production of electromagnetic torque. The starting torque is being used here to display the impedance/torque relation for the two experimental machines – M1 and M2.

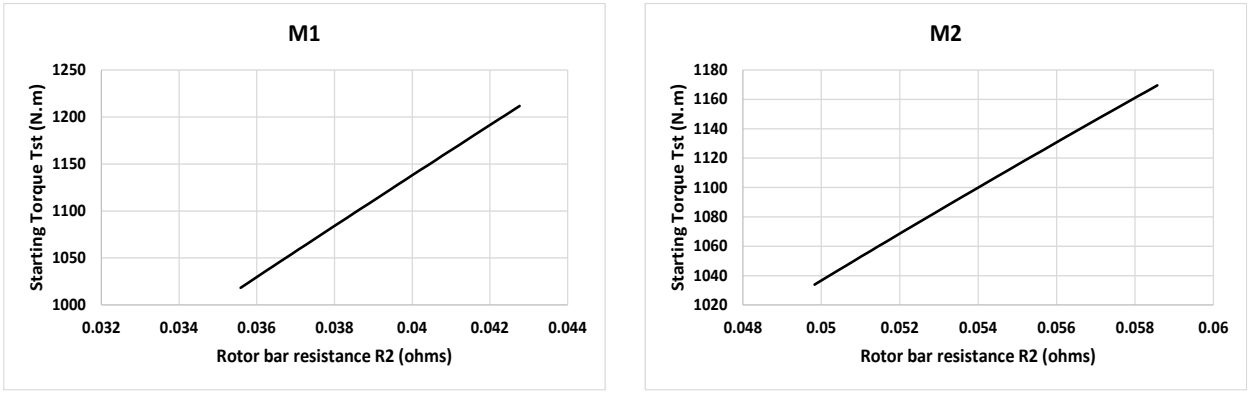

Fig 2: Influence of rotor resistance on high slip torque (Rotor bar of M1 & M2)

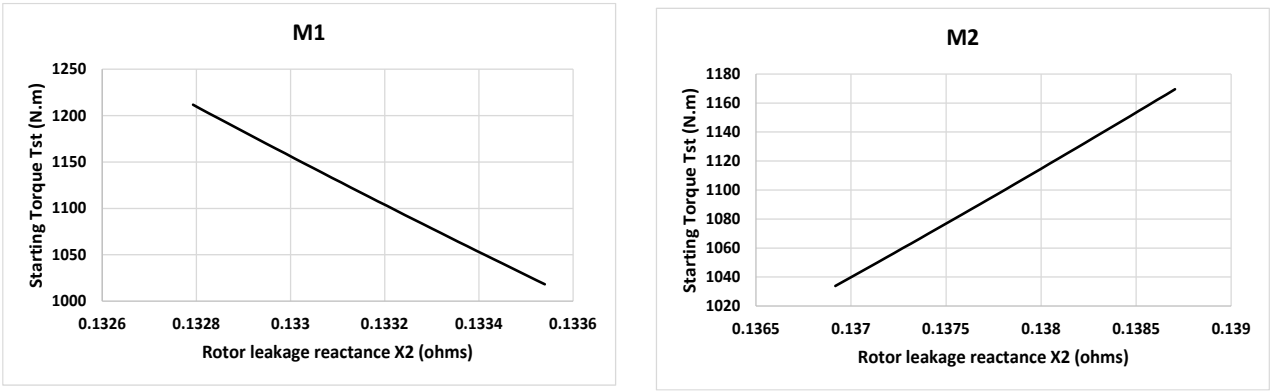

Fig 3: Influence of leakage reactance on high slip torque (Rotor bar of M1 & M2)

But according to [12], the starting torque expression is given as: $T_{ST} = \frac{3p}{2}\frac{R_R}{\omega_e}\left(\frac{U_S}{X_{Ye}}\right)^2$ (1)

In equation 1, U_S is the peak value of the phase voltages, R_R is the rotor resistance, p is the number of pole pairs, ω_e is the frequency of stator voltages, and currents, and reactance X_{Ye} represent the equivalent leakage reactance of the rotor and stator windings of the equivalent two-phase rotor winding that represent the rotor cage and are referred to the stator side.

With all other parameters held constant in equation 1, it may be observed that the relation between the rotor circuit impedance parameters and the starting torque (T_{st}) as depicted by figs 2 and 3, shows substantial agreement with equation 1. However, the reactance/torque relation simulated by M2 in fig 3 is at variance with theory. This seeming oddity is explained in fig 4. As the relevant rotor bar geometry are being altered in M1, it may be observed that first, R_2 is changing much faster than X_2 as the magnitudes of their respective gradients indicate [14]. And second, the individual effect of R_2 (or R_R) and X_2 on T_{st} seems to be mutually aiding (the gradients of R_2 and X_2 are opposite in sense i.e., +ve & -ve). As observed from equation (1), while T_{st} tends to vary directly with R_2, it varies inversely with X_2; so, if the net change in the impedance parameters is to translate into a significant boost in T_{st} for instance, then following a design modification in rotor bar geometry (say a change in the top width of the rotor bar), R_2 has to increase at a faster rate regardless of the direction of change in X_2, or R_2 should increase while X_2 should be dropping. Thus T_{st} grows relatively faster in M1.

Novelty Journals

ISSN 2394-7349

International Journal of Novel Research in Engineering and Science
Vol. 9, Issue 2, pp: (35-39), Month: September 2022 - February 2023, Available at: www.noveltyjournals.com

On the other hand, in M2, though R_2 is also changing much faster than X_2, the individual effect of R_2 and X_2 on T_{st} seems to be against each other (the gradients of R_2 and X_2 are both positive). That is, following a design modification in rotor bar geometry (say a change in the taper angle of the rotor bar), R_2 and X_2 both rise (or fall) together; howbeit the faster rate of change of R_2 tends to prevail, and T_{st} tends to grow as well, but at a relatively slower rate than the M1 case. Whichever the case, it is usually desired that as the T_{st} is being improved, the associated starting current (I_{st}) is curtailed by a large enough rotor impedance that is as resistive as possible. As R_2 is being shored up via the rotor bar geometric design, Fig 5 clearly portrays through the trendline gradients; that the I_{st} was well curtailed (-ve gradient) while T_{st} was simultaneously improving (+ve gradient).

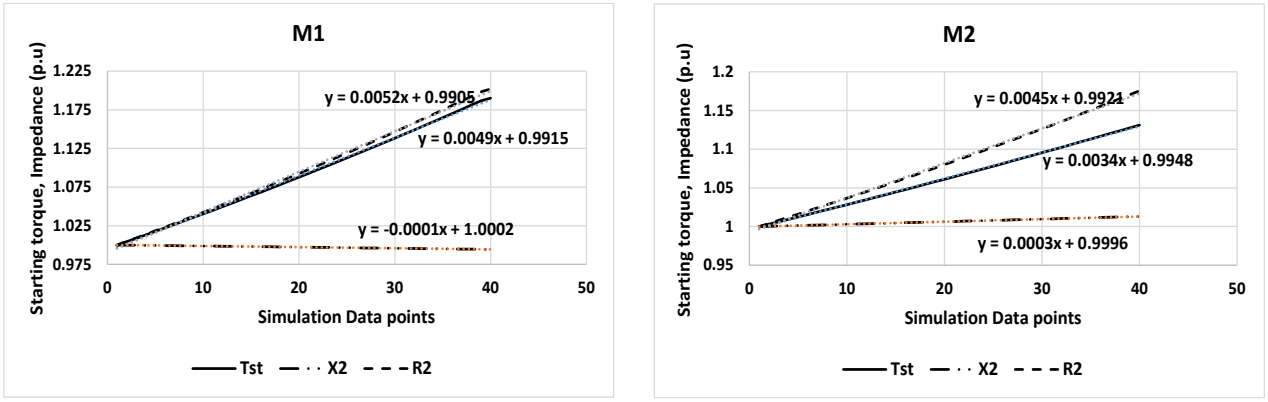

Fig 4: Comparing the relative sensitivity of impedance parameters (Rotor bar of M1 & M2).

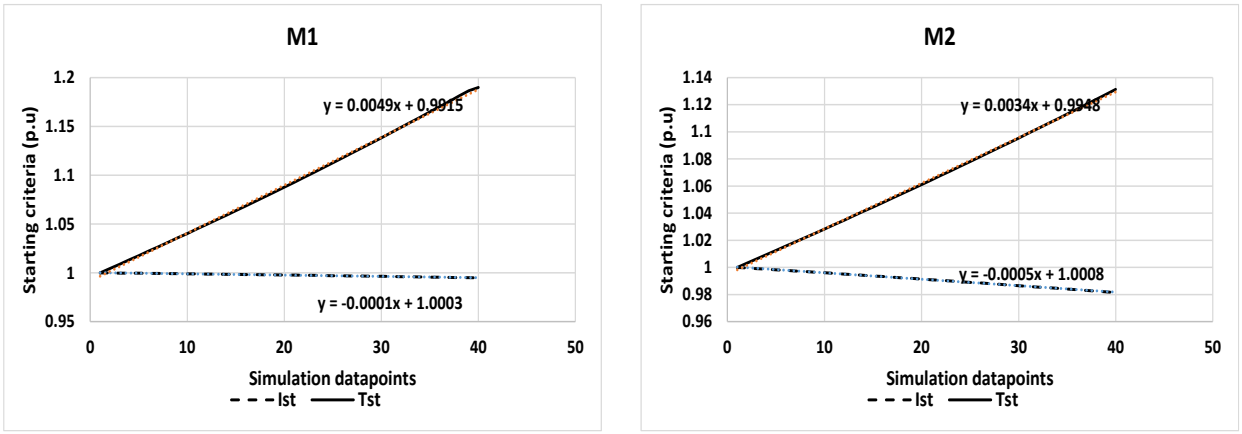

Fig 5: Comparing the growth rate of the starting criteria (Rotor bar of M1 & M2).

Lastly, mathematicians as in [14] have given the equation of a straight line as:

$$y = mx + c. \quad (2)$$

where, m and c are respectively the gradient and y-intercept of the line.

A closer observation of the magnitudes of the coefficient of *x* (the slopes) of the M1 and M2 trendlines of fig 4, indicates the following:

for M1: $\frac{trendline\ gradient\ for\ R_2}{trendline\ gradient\ for\ X_2} = \frac{0.0052}{0.0001} = 52.$

for M2: $\frac{trendline\ gradient\ for\ R_2}{trendline\ gradient\ for\ X_2} = \frac{0.0045}{0.0003} = 15.$

Since 52 is over thrice greater than 15, then the relative sensitivity of the rotor impedance parameters espoused by this paper appears truer for a type M1 rotor shape, compared to a type M2.

IV. CONCLUSION

The major ray of light shed by the above study is that for a given geometric change made to the rotor bar cross section during design or optimization, which tends to influence the standstill values of R_2 and X_2 simultaneously; R_2 appears to be more sensitive to such geometric changes, and consequently seems to be a faster and surer design route to influencing the starting performance in general; compared to X_2. Also, this observed sensitivity seems much stronger for a type M1 rotor shape – one that houses the bulk of the area of its cross section at the bar top. This apparently better sensitivity of R_2 to geometric modifications in the rotor bar, perhaps further justifies the SCIM designer's preference of usually leveraging on R_2, in particular, to influence the starting performance of the motor.

REFERENCES

[1] T. A. Lipo. Introduction to AC Machine Design. New Jersey: IEEE Press, John Wiley & Sons, Inc. PP. 251 – 302. 2017.

[2] H. A. Toliyat and G. B. Kliman. Handbook of Electric Motors. Florida: Taylor & Francis Group. PP. 263 – 265. 2004.

[3] I. Boldea and S. A. Nasar. *The Induction Machine Handbook.* Washington, D.C: CRC Press, Taylor & Francis Group. PP. 447 – 473. 2010.

[4] T. Gönen. *Electrical Machines with Matlab.* New York: Taylor & Francis Group, LLC. Pp. 207 – 262. 2012.

[5] W. R. Finley and M. M. Hodowanec, "Selection of Copper vs. Aluminum Rotors for Induction Motors". Copyright material IEEE. Paper No. PCIC-00-XX. 2000.

[6] H. J. Lee, H. S. Im, D. Y Um, and G. S. Park, "A design of rotor bar for improving starting torque by analyzing rotor resistance and reactance in squirrel cage induction motor". IEEE Transactions on Magnetics. Vol 54. No 3, 8201404. Doi:10.1109/TMAG.2017.2764525. 2017.

[7] P. L. Cochran. *Polyphase Induction Motors. Analysis Design and Application*. Marcel and Dekker. NY. USA. ISBN 0-8247-8043-4. Pp. 427 – 585. 1989.

[8] S. Ho. Analysis and Design of AC Induction Motors With Squirrel Cage Rotors. Doctoral Dissertations. University of New Hampshire, Durham. Retrieved from: https://scholars.unh.edu/dissertation/1909, 1996.

[9] S. J. Chapman. *Electric Machinery Fundamentals. Fourth Edition.* The McGraw-Hill Companies. Inc. ISBN 0-07-246523—9, www.mhhe.oom. Pp. 380 =472. 2005.

[10] O. N. Omogbai, A. E. Anazia and U. E. Anionovo. "Exploring the Influence of Rotor Bar Taper Angle on Breakdown Torque using Machine Learning". International Journal of Advances in Engineering and Management 2023. Vol 5, No 1, pp: 249-255. www.ijaem.net. 2023.

[11] O. N. Omogbai and K. C. Obute. "Investigating the Design Influence of Rotor Bar Taper Angle on the Starting Torque". www.irejournals.com. Vol. 6. No 7. Pp. 197 – 206. 2023.

[12] N. S. Vukosavic. Electrical Machines. Springer New York Heidelberg Dordrecht London. ISBN: 978-1-4614-0400-2 (www.springer.com). DOI: 10.1007/978-1-4614- 0400-2. Pp. 365 – 472. 2013.

[13] J. J. Cathey. Electric machines: analysis and design applying Matlab. New York: McGraw-Hill Higher Education. PP. 317 - 420. 2001.

[14] R. D. Bunday and H. Mulholland. Pure Mathematics for Advanced Level. Second edition. Butterworth & Co Ltd. Great Britain. 1983.